Chem Biol Drug Des 2006; **67:** 155–161

Research Article

doi: 10.1111/j.1747-0285.2006.00348.x

Drug Resistance of HIV-1 Protease Against JE-2147: I47V Mutation Investigated by Molecular Dynamics Simulation

Pradipta Bandyopadhyay* and B. R. Meher

Department of Biotechnology, Indian Institute of Technology, Guwahati, Assam 781 039, India
**Corresponding author: Pradipta Bandyopadhyay, pradipta@iitg.ernet.in*

Anti-retroviral therapies for acquired immunodeficiency syndrome (AIDS) patients are at risk because of drug resistance that has been identified with a number of currently marketed drugs. HIV-1 protease (HIV-pr), a well-validated AIDS therapeutic target, undergoes various mutations leading to resistance such existing drugs. However, the molecular basis of drug resistance of HIV-pr is still not fully understood. JE-2147, an experimental inhibitor of HIV-pr, shows a resistance profile different from that of known drugs. Noteworthy, it is less susceptible to several common mutations, but it is still susceptible to a few mutations, including I47V which appears to be specific for JE-2147. In this work, the molecular details of the effect of I47V mutation is investigated using molecular dynamics simulation. Four simulations of apo and complexed proteins in their wild type (WT) and mutant forms have been performed. It is found that the mobility of the side chain of mutant Val47 in chain B of HIV-pr about the inhibitor increases significantly relative to WT Ile47 in chain B. This is due to loss of optimized packing of the inhibitor to the residue 47 in chain B of the mutant when compared with WT enzyme. There also are subtle differences in motion involving residues in the flap region, which are more prominent in the apo form.

Key words: dihedral angle, drug resistance, HIV protease, molecular dynamics, protein flexibility

Received 17 October 2005, revised 31 December 2005 and accepted for publication 31 December 2005

Acquired immunodeficiency syndrome (AIDS) is caused by HIV-infection and has developed into a major epidemic in the world over recent years. Currently, it is estimated that about 32 million people have died from AIDS, and the infection is spreading at an alarming rate. It is also estimated that there were 4.9 million new HIV infections in 2004 and about 3.1 million people have died from AIDS in 2004 alone (1). UNAIDS projections indicate that an additional 45 million people will be infected in the next decade unless the world succeeds in establishing preventive and/or curative therapies capable of global impact.

As HIV is a retrovirus, its genome is encoded by RNA, which is reverse-transcribed to viral DNA by the viral reverse transcriptase (RT) upon entering a new host cell. This is followed by integration, transcription, translation and finally assembly and budding of HIV-proteins. Anti-HIV drugs have been developed by focusing on key therapeutic targets at different points of the viral life cycle. To date, the Food and Drug administration (FDA) has approved anti-HIV drugs which have inhibitory properties against three different viral proteins, HIV-RT, HIV-protease (HIV-pr) and HIV-gp41. Several HIV-pr inhibitors have achieved FDA approval as a result of intense drug discovery efforts (2–5). Mechanistically, HIV-pr is a member of the aspartyl protease family, and it functions at the late stage of infection by cleaving viral gag and gag-gol polyproteins to generate mature infectious virions. Hence, HIV-pr inhibitors are effective to effect incomplete processing of these virions to produce immature, non-infectious viral particles. Furthermore, HIV-pr inhibitor research has become one of the major success stories of developing drugs using structure-based drug design, including a combination of X-ray crystallography and computational technologies (6).

The HIV-pr is a dimer of which each monomer contains 99 amino acid residues. It has C_2 symmetry in the unbound state, albeit this is lost with the binding of asymmetric ligands. The structure of HIV-pr is shown in Figure 1. Flap (residues 43–58), flap elbow (residues 35–42), fulcrum (residues 11–22), cantilever (residues 59–75), and ligand binding regions are represented. The residues of HIV-pr are numbered as 1–99 and 1′–99′ for each monomer (chain A and B, respectively).

The major problem associated with the existing drugs against HIV-pr is molecular resistance. Such drugs are losing their effectiveness against HIV-pr due to rapid point mutations of the genome of HIV. Two types of mutations have been identified for HIV-pr. One type occurs proximal to the active site and directly affects inhibitor binding by reducing the van der Waals (VDW) contacts, increasing steric hindrance, and/or increasing the number of unfavorable electrostatic interactions between HIV-pr and inhibitors (7). The other type occurs distal to the active site and modifies enzymatic function (8) via conformational changes that increase the affinity of the protease for substrates over inhibitors, the so-called compensatory mutation.

Computational studies have been extremely valuable to investigate the molecular basis of drug resistance and understand both protein

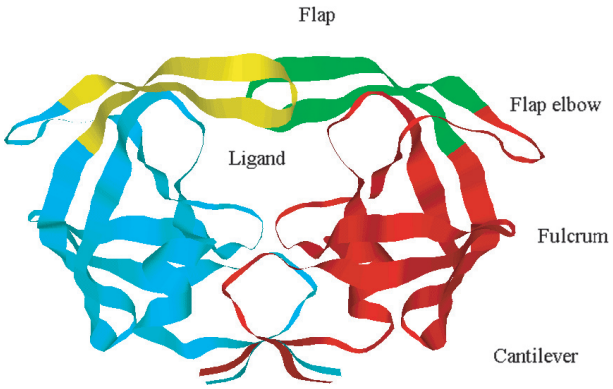

Figure 1: Structure of HIV protease shown as ribbon. Important structural elements (e.g. flap, fulcrum, cantilever and the ligand binding region) are highlighted.

conformational changes and dynamics which are otherwise difficult to address relative to static X-ray structures. Knowledge of minute details of such mutation effects at the atomic level may contribute to hypotheses of drug resistance and drug design with respect to inhibitor modifications that may overcome drug resistance. In the current study, we have focused on a very high-resolution (1.09 Å) crystal structure of HIV-pr complexed with inhibitor JE-2147 (9). This high-resolution structure allows a more detailed analysis into the drug resistance mechanism of HIV-protease. JE-2147, shown in Figure 2, is a peptidomimetic inhibitor developed by scientists at Agouron (Pfizer). *In vitro* data suggest that JE-2147 may be more efficient than currently marketed HIV-pr inhibitors (10, 11). In particular, JE-2147 possesses a unique resistance profile in terms of having two major mutations, namely, I84V and I47V. Interestingly, albeit I84V is a common mutation for other HIV-pr inhibitors, I47V appears to be specific for JE-2147.

Therefore, we have investigated the effect of I47V mutation using molecular dynamics (MD) simulation of both wild type (WT) and mutant HIV-pr with respect to apo or inhibitor complexed protein to gain insight into this complex process. The outcome of these simulations shows that the mobility of the inhibitor is different between WT and mutant HIV-pr, and that mobility of residues in the flap region is different between the WT and mutant HIV-pr especially for the apo protein. Both these effects have implications in drug binding, as flap motion is possibly related to inhibitor binding and a loss of direct molecular interactions between HIV-pr and inhibitor will affect binding free energy. Another objective of this work is to determine if any generalization related to drug resistance of HIV-pr may be made by comparing the results of this study with previously published works.

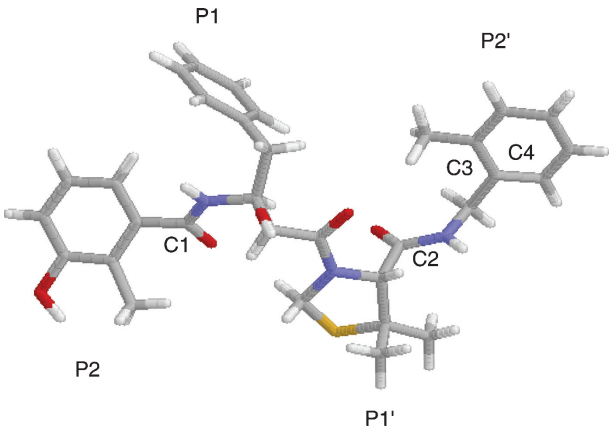

Figure 2: Structure of JE-2147. Atoms H, C, O, N and S are shown in color white, gray, red, blue, and yellow respectively. P1, P2, P1′ and P2′ represent different substructural moieties. Atoms C_1, C_2, C_3 and C_4 define structural parameters (see text for discussion) for analysis.

Methods and Materials

All four MD simulations were started using a high-resolution crystal structure of HIV-pr with JE-2147 (pdb ID 1KZK). The Leap module of AMBER program package (12) was used to prepare the system for the simulation. The AMBER 99 force field was used for the simulation (13). Charges of JE-2147 were calculated using the RESP (14) procedure at the Hartree–Fock level with 6–31G* basis set after minimizing the molecule at the AM1 semi-empirical level (15). All four systems were immersed in a water box of size $83.5 \times 62.5 \times 68.9$ Å^3 containing >8000 water molecules. The TIP3P (16) model was used to represent the water molecules. The net positive charge on the system was neutralized through the addition of chloride ions.

For the simulations of the complexed protein, charged state of the Asp25′ (catalytic aspartate in chain B) was taken as protonated. This is in accord with the finding in reference (17) that Asp25′ was protonated. Detailed calculations (7) for HIV-pr and Saquinavir, a ligand similar to JE-2147 also found that one of the Asp residues is protonated. The electrostatic interactions were calculated with the particle mesh ewald method (18). Constant temperature and pressure conditions in the simulation were achieved by coupling the system to a Berendsen's thermostat and barostat (19). Bonds involving the hydrogen atoms were constrained to their equilibrium position with the SHAKE algorithm. The whole system was minimized for 200 steps. Then the system was heated to 300K over 20 ps with a 1 fs time step. Subsequently, 180 ps MD run was performed for equilibration. The time step for MD simulation for the production run was 2 fs. The system was then run for 3 ns and the stability of the trajectories were carefully monitored and first 300 ps was removed from the analysis. Since there is no structure available for the I47V mutant, 1KZK structure was taken as a template and both Ile47 and Ile47′ residues were replaced by Val.

Results and Discussion

There are a number of attempts to understand drug resistance of HIV-pr using computational techniques. They differ in the particular mutation and inhibitor studied. Moreover, the lengths of MD simulation covered a wide range [600 ps (7) to 22 ns (5)]. Analysis of the MD trajectories was also performed in a variety of ways. The main purpose of the present work is to understand the direct and indirect effects of I47V mutation and compare it with some other known mutations. The following analysis is done keeping that in mind. In particular, the opening of flaps and protein–ligand movements are considered in the analysis.

Stability of the trajectories

The stability of the trajectories of all four simulations was monitored by plotting the RMSD values of the C_α atoms as shown in Figure 3. It was determined that the rmsd of all trajectories were similar from the starting structures during the course of

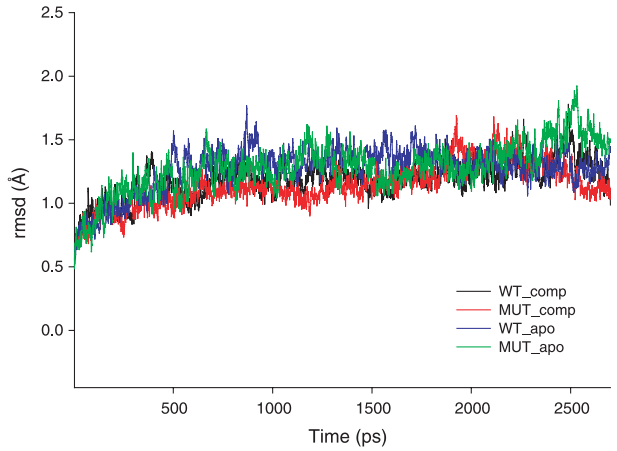

Figure 3: RMSD values for the C_α atoms for wild type (WT) and mutant simulation of both apo and complexed forms.

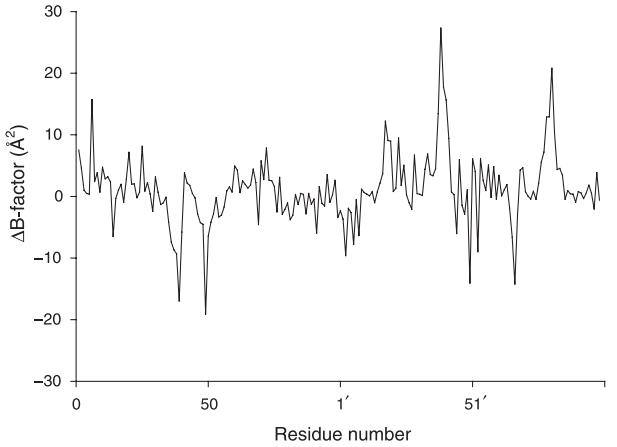

Figure 4: Difference of B-factor values from molecular dynamics (MD) simulation for WT and mutant HIV-pr simulation of the apo protein (mutant B-factor–WT B-factor).

the simulations with values around 1.2–1.6 Å ensuring stable trajectories.

Comparing the apo proteins: WT versus mutant

The difference in isotropic temperature (B) factor between mutant and WT for each residue is shown in Figure 4. A difference of B factors may provide insights into the structural fluctuation of different regions of WT and mutant protein. The maximum changes in B-factor occurs between WT and mutant HIV-pr for the residues in the flap elbows of the two chains (34–35, 37, 35′–41′), flaps of the two chains (48–51, 46′–54′), and part of the cantilever region (65–70, 65′–68′). It is noted that several other regions comparing WT and mutant HIV-pr exist in which B-factors were different. In summary, by comparison of the B-factors between WT and mutant HIV-pr, a difference in the fluctuation of several amino acids was found, and this especially included those residues at the flap tips, flap elbows and cantilever region.

Analysis of local fluctuations of WT and mutant HIV-pr

With respect to local structural differences between WT and mutant HIV-pr, the flap movement is especially important to investigate. It is known that flap dynamics affects both inhibitor binding and enzyme catalysis of HIV-pr. Furthermore, several mutations affect flap dynamics. For example, L90M and V82F/I84V mutations open the flap moreso in the mutant than the WT (5, 20). On the other hand, M46I mutation makes the flap more closed (8). Recently, a very detailed study by McCammon and co-workers on V82F/I84V mutant HIV-pr used a variety of parameters to find the flap dynamics (5). We have used several of these parameters to enquire the extent of flap motion.

Flap tip to active site distance

The distance between the flap tip [C_α of Ile50 (50′)] and catalytic aspartates [C_α of Asp25(25′)] was measured from the simulation and the distributions are shown in Figure 5A and B for chains A and B, respectively. These results reveal that the distance between

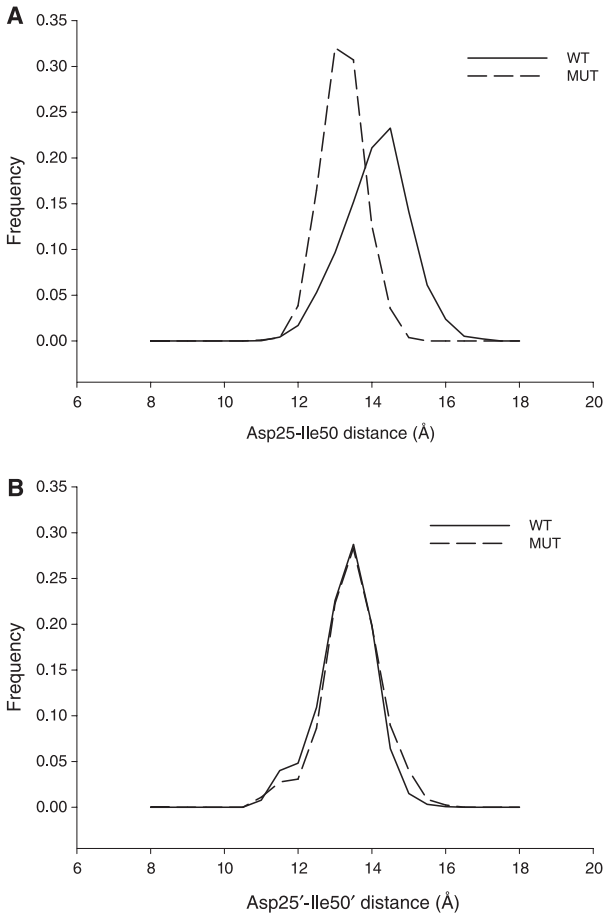

Figure 5: (A) Distributions of Asp25–Ile50 distance for both wild type (WT) and mutant HIV-pr simulation of the apo protein; and (B) distributions of Asp25′–Ile50′ distance for WT and mutant HIV-pr simulation of the apo protein.

flap tip and catalytic site in chain A is clearly different for WT and mutant HIV-pr. The mean of WT distribution is 14.6 Å and standard deviation is 1.0 Å. For the mutant, the mean and standard deviation are 13.5 and 0.6 Å, respectively. Therefore, the mean of these two distributions differ by >1.0 Å and WT distribution covers wider values. However, for chain B, the distributions are almost overlapping. The simulation results suggest that for chain A, the average flap tip to active site distance is less in the case of mutant. A difference in motion of chain A and chain B of HIV-pr has also been observed in other simulation (5).

Ile50 to Ile149 distance

The distance between the C_α of Ile50 and the C_α of Ile149 measures the distance between the flap tips in the two chains and may shed light on the difference of flap motion between WT and mutant HIV-pr (Figure 6). For the mutant, the distribution has one peak around 8 Å, whereas for the WT the main peak is distributed around 7 Å, and two other peaks around 9 and 6 Å. The mean and standard deviation of WT distribution are 7.7 and 0.9 Å and that of mutant are 8.2 and 0.7 Å, respectively. While considerable overlap between the two distributions exist, the distance between the flap tips were determined to fluctuate moreso in the case of WT versus that of the mutant.

The 53′ (C_α) to 67′ (C_α) distance was also monitored (not shown) as large differences in the B-factors for those residues exist. The distributions are found to be different with some overlap. Although the B-factor is quite different for 53′ and 67′, the distance between them was not drastically different for WT and mutant HIV-pr. Likely, this was due to the B-factor for WT HIV-pr was greater for 53′ but less for 67′, hence making the 53′–67′ average distance, on balance, not drastically different in comparing WT and mutant.

Therefore, in analyzing differences in B-factors and the aforementioned computational simulations, the dynamic motion of WT and mutant are different at certain residues. In particular, the distances between residues in the flap elbow and flap tips are dissimilar in the case of mutant and WT.

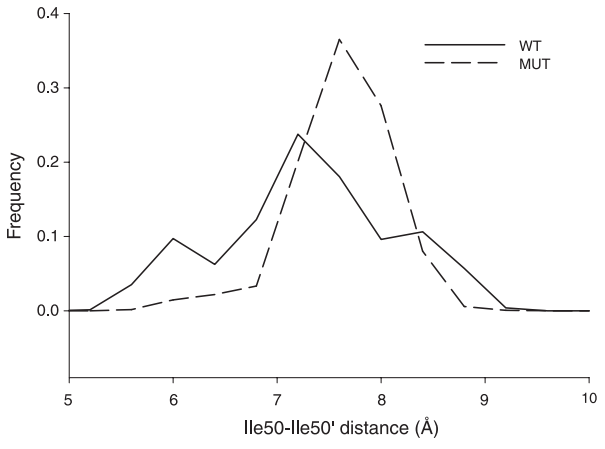

Figure 6: Distributions of Ile50–Ile149 distance for WT and mutant HIV-pr simulation of the apo protein.

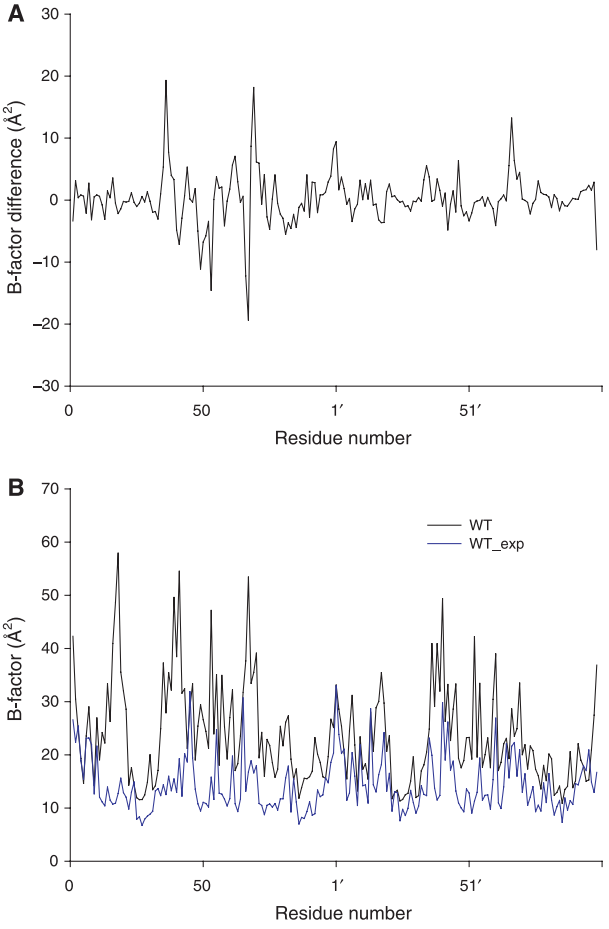

Figure 7: (A) Difference of B-factors for wild type (WT) and mutant complexed HIV-pr (mutant B-factor–WT B-factor); (B) B-factor for the complexed HIV-pr (calculated and experimental results for the WT).

Investigation of the complexed forms of WT and mutant HIV-pr

The difference of temperature factors (B-factor) of the protein in its complexed form is shown in Figure 7A. It can be seen that compared with the apo protein, the difference between WT and mutant is reduced for most of the residues. However, there are significant differences for the residues 36–37 (flap elbow of chain A), 48–52 (flap tips of chain A), 66–69 (66′–69′) (part of the cantilever regions in both chains). Figure 7B shows a comparison between X-ray structure B-factor and calculated B-factor for the WT. The calculated B-factors are much higher than that for the X-ray structure, albeit the general pattern is similar with only few exceptions. It is to be noted that for high-resolution crystal structures (such as the one described in this study) the calculated B-factors can be much higher than that for experimental structures. This finding may be correlated to the fact that high-resolution crystals are typically highly packed and such properties are not included in most simulations (including those performed in this study).

Analysis of local fluctuations of inhibitor complexed WT and mutant HIV-pr

We next investigated several key local fluctuations of inhibitor complexed WT and mutant HIV-pr. These include (a) Asp25(25′)–Ile50(50′) and Ile50–Ile50′ distances which indicate flap and flap-active site movements; (b) Asp25(25′)–inhibitor distance, which will be an indicator of the protein–ligand motion; and (c) dihedral angles of Ile-47′ and the P2′ moiety of the JE-2147 to probe orientation of the protein and inhibitor.

Asp25(25′) to Ile50(50′) and Ile50 to Ile50′ distances

The Asp25(25′)–Ile50(50′) distances were monitored during the course of the simulation to compare with observed differences found in the case of apo proteins. It was found that for chain A the distribution was much narrower compared with the apo proteins. Moreover, the WT and mutant HIV-pr distributions have significant overlap. This indicates that in the inhibitor-bound state, the distance between flap tips and the active site did not differ significantly on mutation for chain A. For chain B, there is greater difference between the distributions when compared with chain A. To probe the relative motion of the flap tips, the Ile50–Ile50′ distance was monitored. The difference between complexed WT and mutant HIV-pr was found to be less and narrower than that of the apo HIV-pr. The results of these studies indicate that although the Ile–Ile distance was similar in complexed HIV-pr there still exists difference in the Asp–Ile distance in chain B. For further analysis of these distributions, refer to Supplementary Materials.

HIV-pr (Asp25/Asp25′) to inhibitor (C_1 and C_2) distance

It has been previously described (21) that the displacement of the substrate to the active site of the protein is coupled with the complex motion of the entire protein. We have used the definition given by Piana *et al.* (8) to obtain the protein–inhibitor distance in a simple manner. Specifically, we determined the average distance between the C_α of the two catalytic Asp (Asp25 and Asp25′) and two carbons of the inhibitor (C_1 and C_2 as shown in Figure 2). The distributions of the average of these four distances (Figure 8) show that WT and mutant HIV-pr are essentially the same, indicating that the inhibitor is bound strongly to the catalytic Asp residues, and mutation has an insignificant effect.

Dihedral angles of HIV-pr Ile47′ and P2′ site of inhibitor

Residue Ile47′ in the WT HIV-pr interacts with the P2′ site of the inhibitor in the crystal structure. The loss of such molecular interactions may be a key direct effect of mutation (10). To explore this, two dihedral angles involving C_β–$C_{\gamma 1}$ ($C_{\gamma 2}$) of Ile-47′ (and Val47′ for the mutant) and C_3–C_4 of JE-2147 (Figure 2) were monitored by simulations to give an indication of relative orientation of the P2′ group of the inhibitor with respect to the side chain of the 47′ residue of HIV-pr. Distributions for the two angles (henceforth denoted by cg1 and cg2) indicated significant differences between the WT and mutant HIV-pr (Figure 9). The dihedral angle measurements for mutant HIV-pr showed a greater fluctuation when compared with that of WT, including values both in the regions near 0° and 360°.

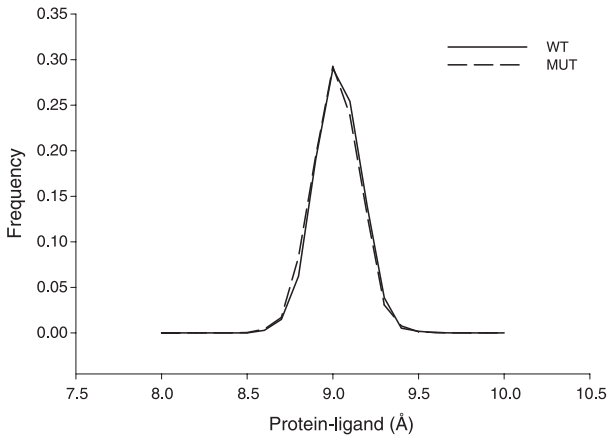

Figure 8: Distributions of protein–inhibitor distances (see text) for both wild type (WT) and mutant HIV-pr simulation.

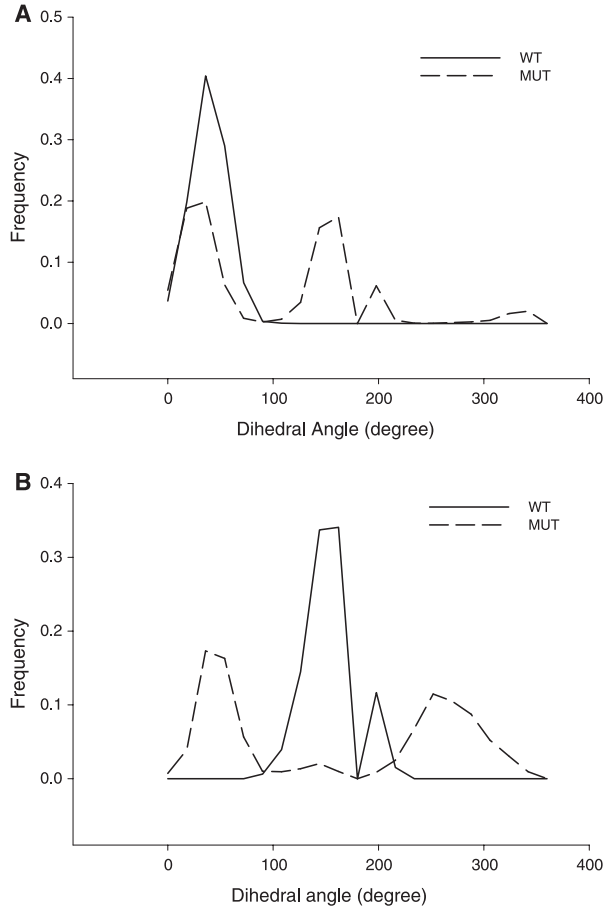

Figure 9: Distributions of dihedral angles (see text) used to obtain orientation of P2′ moiety of the inhibitor relative to the 47′ side chain for both wild type (WT) (A) and mutant (B) HIV-pr simulations.

The mean and Standard Deviation of the WT dihedral angle were 36.5° and 13.9°, respectively, for cg1 and 146.4° and 17.5° for cg2, respectively. The mean and Standard Deviation of the mutant dihedral angles were 134.9° and 138.1°, respectively, for cg1 and 237.6° and 72.2°, respectively, for cg2. Thus, the relative orientation of residue 47′ changes more rapidly and with a wider range of angles relative to the p2′ group in the case of mutant HIV-pr. This results from of the loss of predominantly hydrophobic interaction between the P2′ group of JE-2147 and mutant HIV-pr which effects increased mobility for the inhibitor. Both WT and mutant HIV-pr were analyzed for movement of water molecules, and simulations revealed that only one water molecule came within the 3 Å from the center of the four atoms chosen to define the dihedral angle. Therefore, the effect of water in the direct interaction between 47′ residue of HIV-pr and P2′ of JE-2147 is predicted to be minimal.

Overall molecular analysis of 147V HIV-pr resistance to JE-2147

In this study, drug resistance of 147V HIV-pr against an experimental inhibitor, JE-2147, was investigated to understand the effect of this mutation at the molecular level. For this purpose, four different simulations involving apo and complexed proteins (with and without the 147V mutation) were performed representing all atoms of the protein and inhibitor with thousands of explicit waters. The quality of the simulations were ensured by the rmsd values and by comparing with the B-factor obtained from X-ray for the complexed form of the WT. The results show that for the apo protein, there is difference in dynamic motion of WT and mutant involving the residues in the flap elbow and flap tip regions. In the case of the complexed HIV-pr, the difference in dynamic motion between WT and mutant was less than that of the apo protein relative to the motion of residues in the flaps and flap elbows. The average protein–ligand distance is not affected by mutation. The most distinct motion for the HIV-pr complex was the movement of the side chain of Val47′ about the inhibitor, and this was greater than for Ile47′ in the WT. Hence, such results correlate to losing one $-CH_2$ group in the side chain between mutant and WT proteins, and consequent decreased hydrophobic interactions of Val47′ mutant HIV-pr for inhibitor binding in the case of JE-2147. Such findings suggest that a larger group at the P2′ position JE-2147 might provide recovery of such binding properties. Furthermore, the Val47′ mutation causes a change in the dynamics of the flaps and such disruptions are likely to play a role in the binding and hence to the resistance.

A comparison of the 147V mutation with other studies focused on different mutations is important to further interpret the findings described in this study. In this regard, we have considered the mutations G48V (flap region) and I84V (active site) to compare with I47V. The G48V mutation has been found for the clinical inhibitor Saquinavir (SQV), whereas I84V mutation exists for all clinical inhibitors. It is known that the major direct effect of G48V mutation is increased steric effect between protein and inhibitor (7), whereas the I84V mutation effects the dynamical motion of the protein.

The highly conserved flap tips of HIV-pr I47–G48–G49–I50–G51–G52–F53 are extremely flexible. Nuclear magnetic resonance (NMR) studies by Torchia and colleagues (22) have shown that residues 49–52 have rapid motion in <10 ns time scale and fluctuation of F53 is likely coupled to the motion of the entire flap. Such G48V simulation studies (7) have determined that there is difference in rmsd for the residues in this region upon mutation. It is noted that these reported (7) simulations were performed with complexed HIV-pr, whereas in the present study simulation were conducted with both apo and complexed HIV-pr. It is likely that simulation studies of apo forms of G48V mutation would show more differences in flap motion, and such a finding has been verified in a recent report (23) wherein accelerated MD calculations showed decreased flap motion in the G48V (apo form) to be substantially different from the WT. In the present study, we conclude both direct effects (VDW and steric for residues 47 and 48, respectively) and indirect effects (change of flap dynamics) are functionally involved. For the I84V mutation, the key effect is the dynamical motion of the protein. An examination of the V82F/I84V double mutant shows that it becomes more flexible (the change is much more than the I47V mutant). This would likely compromise inhibitor binding, since a large enthalpic cost would be necessary to close the mutant flap.

Concluding remarks

Unquestionably, the understanding of the molecular basis of drug resistance is a complex task. The specific details obviously depend on position, mutation and the particular inhibitor involved. Nevertheless, the outcome of this study as well as previous studies on HIV-pr provide evidence for both direct effects (i.e. protein residues in the active site) and indirect effects (e.g. protein residues in the mobile flap region).

Acknowledgements

P.B. is grateful to Profs I.D. Kuntz, Prasanta Bandyopadhyay, S. Nandi and Dr W. Arnold. He thanks Dr R. Punekar for checking the English of this paper. He is indebted to the staffs of CDAC-Bangalore and the Supercomputing Facility for Bioinformatics and Computational Biology, IIT Delhi, where most of the calculations were performed. This work is funded by a Department of Science and Technology (DST) fast-track grant (SR/FT/L-43/2004) awarded to P.B.

References

1. UNAIDS (2004): www.unaids.org
2. Swain A., Miller M.M., Green J., Rich D.H., Schneider J., Kent S.B., Wlodawer A. (1990) X-Ray crystallography Structure of a complex between a symthetic protease of Human Immunodeficiency virus 1 and a substrate based Hydroxyethylamine inhibitor. Proc Natl Acad Sci;87:8805.
3. Thaisrivongs S., Skulnick H.I., Turner S.R., Strohback J.W., Tommasi R.A., Johnson P.D., Aristoff P.A., Judge T.M., Gammill R.B., Morris J.K. et al. (1996) Structure-based design of HIV protease inhibitors: sulfonamide-containing 5,6-dihydro-4-hydroxy-2-pyrones as non-peptide inhibitors. J Med Chem;39:4349.
4. Wang W., Kollman P.A. (2000) Free energy calculations on dimer stability of the HIV protease using molecular dynamics and a continuum solvent model. J Mol Biol;303:567.
5. Perryman A.L., Mccammon J.H., Lin J.A. (2004) HIV-1 protease resistance molecular dynamics of a wild-type and of the V82F/I84V mutant: Possible contributions to drug resistance and a potential new target site for drugs. Protein Sci;13:1108.
6. Wlodawer A., Vondrasek J. (1998) Inhibitors of HIV-1 protease: a major success of structure-assisted drug design annu. Rev Biomol Struc;27:249.

7. Wittayanarakul K., Aruksakumwong O., Saen-oon S., Chantratita W., Parasuk V., Sompompisut P., Hannongnua S. (2005) Insights into saquinavir resistance in the G48V HIV-1 protease: quantum calculations and molecular dynamics simulations. Biophys J;88:867.
8. Piana S., Carloni P., Rothlishberger U. (2002) Drug resistance in HIV-1 protease: flexibility-assisted mechanism of compensatory mutations. Protein Sci;11:2393.
9. Reiling K.K., Endres N.F., Dauber D.S., Craik C.S., Stroud R.M. (2002) Anisotropic dynamics of the JE-2147-HIV protease complex: drug resistance and thermodynamic binding mode examined in a 1.09 A structure. Biochemistry;41:4582.
10. Yoshimura K. et al. (1999) JE-2147: a dipeptide protease inhibitor (PI) that potently inhibits multi-PI-resistant HIV-1. Proc Natl Acad Sci;96:8675.
11. Ohtaka H., Schon A., Freire E. (2003) Multidrug resistance to HIV-1 protease Inhibition requires cooperative coupling between distal mutations. Biochemistry;42:13659.
12. Case D.A. et al. (???) AMBER 7. San Francisco, CA: University of California.
13. Cornell W.D., Cieplak P., Bayly C.L., Gould L.R., Merz K.M., Ferguson D.M., Spellmeyer D.C., Fox T., Caldwell J.W., Kollman P.A. (1995) A second generation force field for the simulation of proteins, nucleic acids, and organic molecules. J Am Chem Soc;117:5179.
14. Bayly C.L., Cieplak P., Cornell W.D., Kollman P.A. (1993) A well-behaved electrostatic potential based method using charge restraints for determining atom-centered charges: the RESP model. J Phys Chem;97:10269.
15. Dewar M.J.S., Zoebisch E.G., Healy E.F., Stewart J.P. (1985) Development and use of quantum mechanical molecular models. 76. AM1: a new general purpose quantum mechanical molecular model. J Am Chem Soc;107:3902.
16. Jorgensen W.L., Chandrasekhar J., Madura J.D. (1983) Comparison of simple potential functions for simulating liquid water. J Chem Phys;79:926.
17. Wang Y., Freedberg D.I., Yamazaki T., Wingfield P.T., Stahl S.J., Kaufman J.D., Kiso Y., Torchia D.A. (1996) ????. Biochemistry;35:9945.
18. Essmann U., Pereea L., Berkowitz M.L., Darden T. (1995) A smooth particle mesh ewald method. J Chem Phys;103:8577.
19. Berendsen H.J.C., Postma J.P.M., Van Gunsteren W.F., Dinola A., Haak J.R. (1984) Molecular dynamics with coupling to an external bath. J Chem Phys;81:3684.
20. Maschera B., Darby G., Palu G., Wright L.L., Tisdale M., Myers R., Blair E.D., Fufine E.S. (1996) Human immunodeficiency virus: mutations in the viral protease that confer resistance to saquinavir increase the dissociation rate constant for of the protease-saquinavir complex. J Biol Chem;271:33231.
21. Piana S., Carloni P., Parrinello M. (2002) Role of conformational fluctuations in the enzymatic reaction of HIV-1 protease. J Mol Bio;319:567.
22. Ishima R., Freedberg D.I., Wang Y.X., Louis J.M., Torchia D.A. (1999) Flap opening and dimer-interface flexibility in the free and inhibitor-bound HIV protease, and their implications for function. Struct Fold Des;7:1047.
23. Hamelberg D., McCammon J.A. (2005) Fast peptidyl cis-trans isomerization within the flexible Gly-rich Flaps of HIV-1 Protease. J Am Chem Soc;127:13778.

Supplementary Material

Figure 1: Distributions of Asp25–Ile50 distance for both wild type (WT) and mutant simulation of complexed HIV-pr.

Figure 2: Distributions of Asp124–Ile149 distance for both wild type (WT) and mutant simulation of complexed HIV-pr.

Figure 3: Distributions of Ile50–Ile149 distance for both wild type (WT) and mutant of complexed HIV-pr.